4×130 Gbit/s PS-PAM-16 Transmissions Using an Integrated SOA-PIN Design for Intra-DCIs Enabled by Machine Learning

Ahmed Galib Reza(1), Lakshmi Narayanan Venkatasubramani(1), Anil Raj Gautam(1), Marcos Troncoso-Costas(1,2), Mihail Raytcheva(3), Ahmad Atieh(3) and Liam P. Barry(1)

(1) School of Electronic Engineering, Dublin City University, Dublin 9, Ireland, ahmed.galibreza@dcu.ie
(2) AtlanTTic Research Center, University of Vigo, EI Telecommunication, 36310 Vigo, Spain
(3) Optiwave Systems Inc., Ottawa, Ontario, K2E 8A7, Canada

Abstract *This paper reports the first experimental demonstration of 4×130 Gbit/s probabilistically shaped PAM-16 transmission over 1km using an integrated SOA-PIN design for next-generation intra-DCIs. With a T-spaced neural network equalizer, a BER below the SD-FEC threshold is achieved under a 20-GHz bandwidth limit. ©2023 The Author(s)*

Introduction

Explosive demand for data due to the relentless growth of the Internet of Things (IoT), cloud-based services, social networking, and so on, is driving the need for a capacity expansion of data center interconnects (DCIs) [1]. As the intensity-modulation and direct-detection (IM/DD) technology is the most promising candidate for DCIs [2], many previous reports on DCIs are based on higher-order modulation formats such as PAM-4, PAM-8, etc., to enhance data rate with limited bandwidth [3,4]. Wavelength division multiplexing (WDM) techniques or the installation of parallel fibers can also increase the transmission capacity [2,5].

Since the higher-order modulation formats are more prone to distortions, various digital signal processing (DSP) techniques are proposed, such as feed-forward equalizer (FFE), Volterra nonlinear equalizer (VNLE), decision feedback equalizer (DFE), machine learning (ML), etc., to overcome the bandwidth limitations of the transmission system, chromatic dispersion, nonlinear response of the modulators, and fiber nonlinearity [6-10]. Recently, probabilistic shaping (PS) has been investigated for short-reach IM/DD systems and has shown resilience against noise and nonlinear distortions, especially with PAM-8, and PAM-16 [11-15].

Previous reports on PS-PAM-16 [13-15] for DCIs only studied high-speed single-lane transmissions and considered an erbium-doped fiber amplifier (EDFA) in the system, not suitable for DCI applications from the perspective of cost, size, and energy consumption. Furthermore, studying the performance of such systems in a WDM scenario is critically required, as a WDM transmission system may suffer from the supplementary penalty due to fiber nonlinearity such as four-wave mixing (FWM), and cross-phase modulations (XPM) [16].

In this paper, for the first time, to the best of our knowledge, we experimentally demonstrate 4-λ PS-PAM-16 transmissions with a per channel transmission capacity of 130 Gbit/s under a 20-GHz bandwidth limit across the C-band in the DWDM grid. Due to the low sensitivity of a PIN receiver and lack of a wide-band avalanche photodetector, we utilize the notion of a monolithically integrated semiconductor optical amplifier (SOA)-PIN receiver module to improve the sensitivity of the transmission system [17], critically required for the application of high-order modulation formats and WDM systems. With a low-complexity T-spaced artificial neural network (ANN) equalizer, we report the BER results at the soft-decision forward error correction (SD-FEC) limit of 1.2×10^{-2} [18] after 1 km transmission by using a low-biased SOA, enabling an energy-efficient receiver design and DSP circuitry.

Experimental Setup

The experimental setup for 4-λ PS-PAM-16 transmissions on the DWDM grid with a channel spacing of 1.6 nm is illustrated in Fig. 1. Four narrow linewidth external cavity lasers (ECLs), tunable over a wavelength range of 1527.6 nm – 1568.6 nm, each of which produces an optical output power of about 15 dBm are utilized in the experiment. The respective ECL outputs are sent to the four polarization controllers (PCs) to independently adjust the polarization state of light before being combined by a 4×1 passive optical combiner to generate a 200-GHz spaced 4-λ DWDM channel. The combined laser outputs are modulated by a Mach-Zehnder modulator (MZM).

At the transmitter, the Maxwell-Boltzmann (MB)-distributed PS-PAM-16 signals with a sequence length of 2^{16} are generated in MATLAB by using a lookup table. In Fig. 1(a), the histogram of PS-PAM-16 symbols with an entropy of 3.4690 bits/symbol is presented. Next, the 37.5 GBaud PS-PAM-16 symbols are upsampled, pulse-shaped using a root-raised

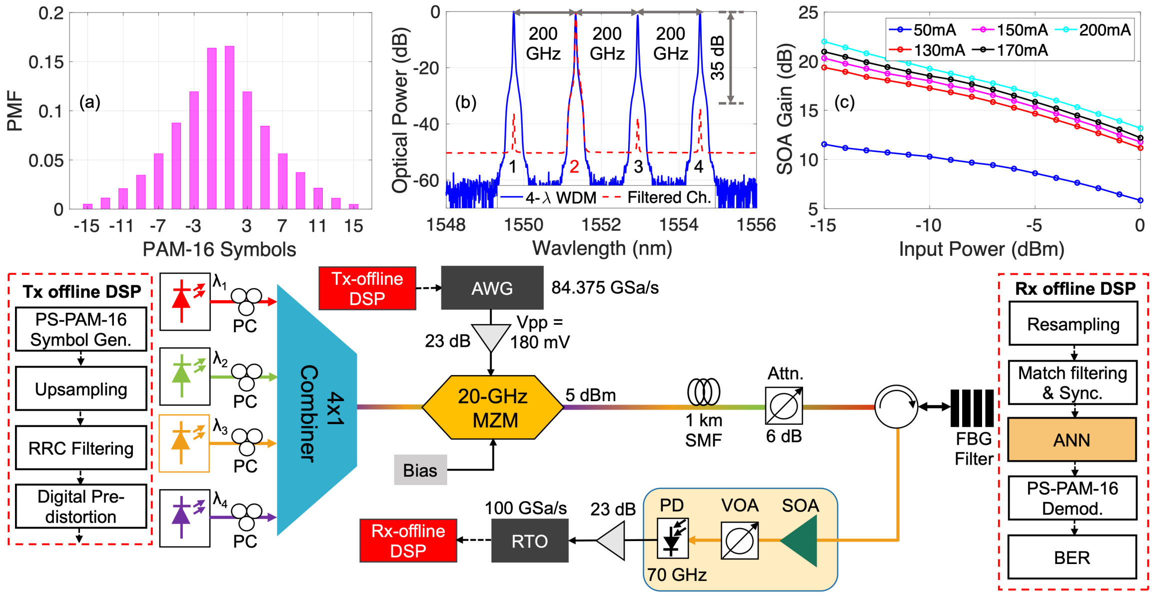

Fig. 1: Experimental setup for 4×130 Gbit/s PS-PAM-16 transmissions over 1 km. (a) Histogram of PS-PAM-16 symbols. (b) Optical spectra after 1 km before (blue) and after demultiplexing (red). (c) SOA gain as a function of the input power.

cosine (RRC) filter with a roll-off factor of 0.1, and digitally pre-distorted to account for the nonlinear responses of the MZM. Now, the digital PS-PAM-16 symbols are loaded to a 32-GHz arbitrary waveform generator (AWG) running at 84.375 GSa/s. The AWG output voltage of 180 mV is amplified using a 55-GHz RF amplifier with a gain of 23 dB, which drives the 20-GHz quad-biased MZM. Upon modulation, we can note a total modulated output power of about 5 dBm (≈-1 dBm/channel), which is launched into a 1 km single-mode fiber (SMF).

After transmission, we demultiplex a WDM channel by using a three-port optical circulator and a fiber-compatible, low-cost, and low-loss fiber Bragg grating (FBG) filter with a fixed central wavelength of 1551.319 nm of the reflected band, providing a suppression ratio of 35 dB, as shown in Fig. 1(b). The 4-λ spectra in Fig. 1(b) after 1 km confirms that due to a low launch power of 5 dBm into the fiber, the system penalties owing to FWM, and XPM are not of concern. A 6 dB optical attenuator is placed in the system before the circulator to account for the splitter loss. The optical signal power after wavelength demultiplexing is about -9 dBm, which is amplified with an SOA to improve sensitivity. From the SOA gain curve presented in Fig. 1(c) for various input power and bias currents, we find that the 3 dB saturation input power changes according to the SOA bias current. Next, the received optical power (ROP) is adjusted with a variable optical attenuator (VOA) and detected by a 70-GHz photodetector before the signal is amplified with a 55-GHz RF amplifier (23 dB gain) and captured using a 33-GHz real-time oscilloscope (RTO) operating at 100 GSa/s for offline DSP. Subsequently, we apply matched-filtering, resampling to 1 sample/symbol, symbol synchronization, and ML-based nonlinear equalization using an ANN consisting of 20 input nodes, a hidden layer of 20 nodes, and 1 output node. As for the activation functions, the logistic sigmoid and linear functions are used in the hidden and output layers of the ANN, respectively. Lastly, after demodulation of the PS-PAM-16 symbols, the bit error ratio (BER) performance is obtained through error counting.

Experimental Results

In Fig. 2(a), the relative intensity noise (RIN) spectrum of the ECL for the wavelength of 1551.319 nm is presented. The ECL exhibits a flat RIN spectrum over the frequency range of DC - 20 GHz with a low average RIN value of about -155 dBc/Hz, which enables the ECL for the transmission of higher-order modulation formats, such as PAM-8, PAM-16, etc.

In Fig. 2(b), the equalized BERs of 4×37.5 GBaud PS-PAM-16 at ROP = 2 dBm after 1 km transmissions for three different entropies of 3.877, 3.689, and 3.469 bits/symbol are shown. The entropies are tuned by adjusting the probability of PAM-16 symbols according to the MB distribution. In the plot, a 35-tap feed-forward equalizer (FFE) is applied, and the filter tap size is optimized for the best BER result. We can see that the SD-FEC BER level cannot be reached for any entropy values. However, a significant improvement in the BER is observed as the entropy goes down, even though the required bandwidth remains the same. It implies that the SOA-induced gain saturation and amplified spontaneous emission (ASE) noise might have

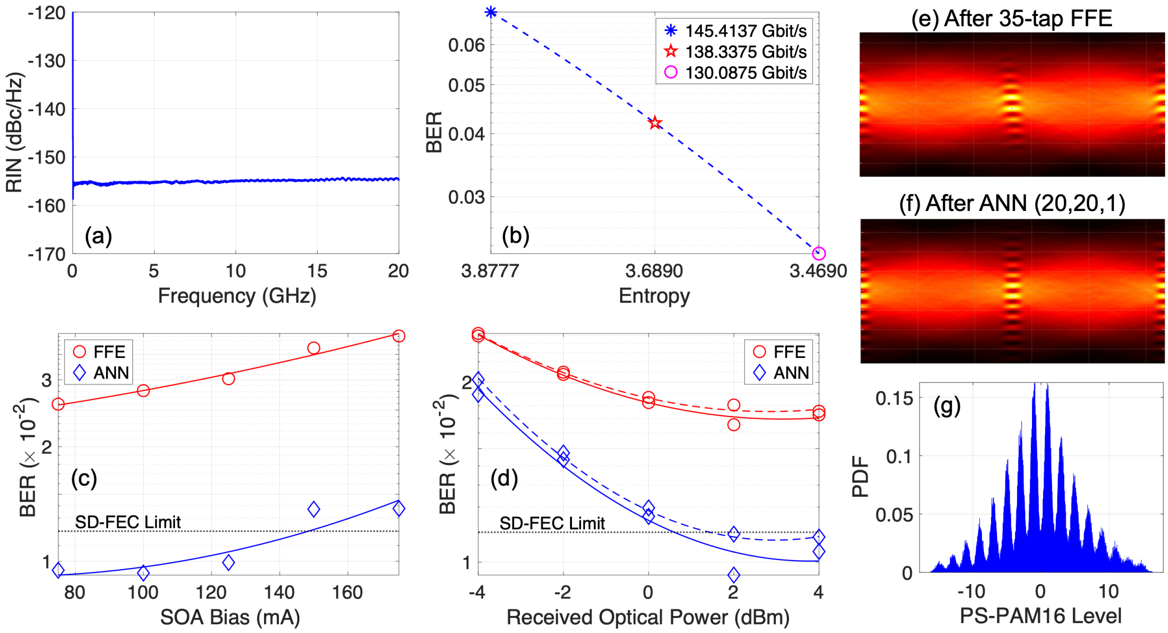

Fig. 2: Experimental results for 4×130 Gbit/s PS-PAM-16 transmissions after 1 km. (a) RIN spectra of the ECL for the wavelength of 1551.319 nm. (b) BER after FFE versus various entropies at ROP = 2 dBm. (c) BER versus SOA bias currents at ROP = 2 dBm. (d) BER versus ROP for the middle (solid line) and edge channels (dash line) after FFE and ANN. Eye diagrams for the middle channel at ROP = 2 dBm after (e) FFE, and (f) ANN. (g) Histogram for the middle channel at ROP = 2 dBm after ANN.

governed the performance. Therefore, a nonlinear equalizer such as ANN can be useful, as it has been found effective against nonlinear distortions [10]. Finally, we pick an entropy of 3.4690 bits/symbol for the next experiments studying the performance and target data rate that employ either an FFE or ANN.

Fig. 2(c) shows the BERs after 35-tap FFE and ANN (20,20,1) versus SOA bias currents after 1 km at ROP = 2 dBm. We see that the ANN completely outperforms the FFE and can reach the SD-FEC level BER of 1.2×10^{-2}. The BER trend line indicates a detrimental effect at higher SOA bias currents due to increased ASE noise and saturated gain. With a bias current of ≥ 150 mA, a BER below the SD-FEC limit cannot be obtained with an ANN. Therefore, in a monolithically integrated SOA-PIN receiver module, a low-biased SOA can limit the nonlinear penalties and enhance the system capacity as well as receiver sensitivity by about 11-12 dB for a minimal increase in power consumption and DSP complexity.

Fig. 2(d) shows the BERs versus ROPs after 4×130 Gbit/s PS-PAM-16 transmissions over 1 km. By tuning the wavelength of the ECLs, two 1.6 nm spaced WDM channels called middle (solid line) and edge channels (dashed line) are demultiplexed by using a fixed wavelength FBG filter (1551.319 nm). In the experiment, the SOA is biased at 75 mA. We observe that the FFE performs poorly due to strong nonlinear distortions for any ROPs. With an ANN equalizer, such distortions can be mitigated and the BERs $< 1.2\times10^{-2}$ can be reached for both middle and edge channels at an ROP = 0.6 and 1.3 dBm, respectively. In Figs. 2(e) and 2(f), the eye diagrams are shown after FFE and ANN at an ROP of 2 dBm, respectively. As expected, the ANN provides a larger de-skewed eye-opening in comparison with an FFE, indicating its effectiveness in mitigating nonlinear signal distortions. Fig. 2(g) presents a histogram plot of the equalized PS-PAM-16 symbols for the middle channel at an ROP of 2 dBm, in which non-overlapping and distinctive PAM-16 symbols are observed after ANN.

Conclusions

We report 4×130 Gbit/s PS-PAM-16 transmissions across the C-band DWDM grid over 1 km SMF under a 20-GHz bandwidth limit for intra-DCIs and present a BER performance within the SD-FEC limit. We found that the PS can enable the transmission of higher-order modulations. Also, with a low-biased SOA-PIN design (suitable for potential integration), we can boost the sensitivity with minimal power consumption and experience minimal distortions for higher-order signals, which can be mitigated with a low-complexity ANN. In summary, the receiver design and DSP techniques studied in this work can offer a viable solution for the development of high-speed DCIs.

Acknowledgements

This work was supported in part by the SFI under Grants 18/SIRG/5579, 13/RC/2077_P2, 12/RC/2276_P2, 18/EPSRC/ 3591, and in part by Enterprise Ireland under Grant DT 2019 0014A.

References

[1] X. Zhou, R. Urata, and H. Liu, “Beyond 1 Tb/s intra-data center interconnect technology: IM-DD or coherent?,” *Journal of Lightwave Technology*, vol. 38, no. 2, pp. 475-484, 2020, DOI: https://doi.org/10.1109/JLT.2019.2956779.

[2] IEEE P802.3bs: 200 Gb/s and 400 Gb/s ethernet task force. [Online] https://www.ieee802.org/3/bs/.

[3] H. Taniguchi, S. Yamamoto, A. Masuda, Y. Kisaka and S. Kanazawa, “800-Gbps PAM-4 2-km transmission using 4−λ LAN-WDM TOSA with MLSE based on deep neural network,” *2022 Optical Fiber Communication Conference and Exhibition (OFC)*, San Diego, United States, 2022, paper Th2A.25, DOI: https://doi.org/10.1364/OFC.2022.Th2A.25.

[4] F. Yang, X. Fang, X. Chen, Y. Li and F. Zhang, “Up to 360 Gb/s optical interconnects with ultra-high bandwidth thin film lithium niobate modulator,” *2022 Optical Fiber Communication Conference and Exhibition (OFC)*, San Diego, United States, 2022, paper M4H.5, DOI: https://doi.org/10.1364/OFC.2022.M4H.5.

[5] S. M. R. Motaghiannezam, “Optical PAM4 Signaling and System Performance for DCI Applications,” *2019 Optical Fiber Communications Conference and Exhibition (OFC)*, San Diego, CA, USA, 2019, paper M3A.1., DOI: https://doi.org/10.1364/OFC.2019.M3A.1.

[6] S. Hu, J. Zhang, J. Tang, Q. Liu, W. Jin, Z. Zhong, R. Giddings, J. Zhou, T. Jin, X. Zhao, B. Xu, X. Gao, and K. Qiu, “112-Gb/s PAM-4 IM/DD optical transmission over 100-km single mode fiber with linear equalizer”, *2022 Optical Fiber Communications Conference and Exhibition*, San Diego, United States, 2022, paper M2H.5, DOI: https://doi.org/10.1364/OFC.2022.M2H.5.

[7] L. Xue, R. Lin, J. V. Kerrebrouck, L. Yi, J. Chen and X. Yin, “100G PAM-4 PON with 34 dB power budget using joint nonlinear Tomlinson-Harashima precoding and Volterra equalization”, *2021 European Conference on Optical Communication (ECOC)*, Bordeaux, France, 2021, pp. 1-4, DOI: https://doi.org/10.1109/ECOC52684.2021.9606041.

[8] J. Zhang, X. Wu, L. S., J. Liu, A. P. T. Lau, C. Guo, S. Yu, and C. Lu, “C-band 120-Gb/s PAM-4 transmission over 50-km SSMF with improved weighted decision-feedback equalizer,” *Optics Express*, vol. 29, no. 25, pp. 41622-41633, 2021, DOI: https://doi.org/10.1364/OE.444231.

[9] A. G. Reza, M. Troncoso-Costas, L. P. Barry, and C. Browning, “4x75-Gbit/s optically amplified WDM-PON with beyond 31-dB power budget employing PAM-4 transmission and a recurrent neural network,” *2022 European Conference on Optical Communication (ECOC)*, Basel Switzerland, 2022, paper Tu1C.2.

[10] A. G. Reza and J. K. Rhee, “Nonlinear equalizer based on neural networks for PAM-4 signal transmission using DML,” *IEEE Photonics Technology Letters*, vol. 30, no. 15, pp. 1416-1419, 2018, DOI: https://doi.org/10.1109/LPT.2018.2852327.

[11] X. Li, Z. Xing, M. S. Alam, M. Jacques, P.-C. Koh, and D. V. Plant, “Cost-minimizing distribution matching supporting net 800 Gbit/s PS-PAM transmission over 2 km using a 4-λ EML TOSA,” *Optics Letters*, vol. 45, no. 17, pp. 4718-4721, 2020, DOI: https://doi.org/10.1364/OL.395631.

[12] A. G. Reza, M. T. Costas, C. Browning, and L. Barry, “124.8-gbit/s net data rate capacity for IM/DD optical intra-data center interconnections by utilizing probabilistically shaped pam-8 and digital linear feed-forward equalizers”, *2022 Asia Communications and Photonics Conference (ACP)*, Shenzhen, China, 2022, pp. 997–1000, DOI: https://doi.org/10.1109/ACP55869.2022.10088965.

[13] X. Chen, J. Cho, G. Raybon, D. Che, K. W. Kim, E. Burrows, P. Kharel, C. Reimer, K. Luke, L. He, and M. Zhang, “Single-wavelength and single-photodiode 700 Gb/s entropy-loaded PS-256-QAM and 200-GBaud PS-PAM-16 transmission over 10-km SMF,” *2020 European Conference on Optical Communications (ECOC)*, Brussels, Belgium, 2020, pp. 1-4, DOI: https://doi.org/10.1109/ECOC48923.2020.9333201.

[14] J. Zhang, X. Wu, Q. Yan, H. Tan, X. Hong, C. Fei, Alan P. T. Lau, and C. Lu, “Nonlinearity-aware PS-PAM-16 transmission for C-band net-300-Gbit/s/λ short-reach optical interconnects with a single DAC,” *Optics Letters*, vol. 47, no. 12, pp. 3035-3038, 2022, https://doi.org/10.1364/OL.462013.

[15] X. Wu, J. Zhang, Q. Yan, A. Pak Tao Lau and C. Lu, “C-band single-lane 290.4-Gb/s net rate PS-PAM-16 transmission over 1-km SSMF using low-complexity nonlinear equalization and single DAC,” *2022 Conference on Lasers and Electro-Optics (CLEO)*, San Jose, CA, USA, 2022, paper SM3J.6, DOI: https://doi.org/10.1364/CLEO_SI.2022.SM3J.6.

[16] J. D. Reis, D. M. Neves, and A. L. Teixeira, “Analysis of nonlinearities on coherent ultradense WDM-PONs using Volterra series,” *Journal of Lightwave Technology*, vol. 30, no. 2, pp. 234-241, 2012, DOI: https://doi.org/10.1109/JLT.2011.2180698.

[17] C. Caillaud, P. Chanclou, F. Blache, P. Angelini, B. Duval, P. Charbonnier, D. Lanteri, G. Glastre, and M. Achouche, “Integrated SOA-PIN detector for high-speed short reach applications,” in *Journal of Lightwave Technology*, vol. 33, no. 8, pp. 1596-1601, 2015, DOI: https://doi.org/10.1109/JLT.2015.2389533.

[18] International Telecommunication Union (ITU-T) G.709.2/ Y.1331.2 recommendation, 07/2018. [Online] https://www.itu.int/rec/T-REC-G.709.2/en.